1

General Points

1.1. Introduction

This book is the continuation of [TAR 11a] and [TAR 11b]. The series as a whole gives a broad-ranging presentation of the statistical properties of turbulent flows delimited by rigid walls. It is preferable, though not obligatory, for the readers to consult [TAR 11a] and [TAR 11b]. This chapter lays out the basic elements and the literature necessary for the understanding of this book. We limit ourselves to give an overview as brief as possible, without going into details, which the interested readers can find out in numerous publications referenced herein.

First, we provide a summary of the fundamental equations in fluid dynamics (the Navier–Stokes (NS) momentum balance equations and the conservation of mass equations). We then proceed to discuss the Reynolds-averaged equations. We lay down a number of exact solutions related to fully developed turbulent flows in a two-dimensional (2D) channel, before providing a brief reminder about turbulent boundary layers and their overall characteristics. Wall turbulent scales are then introduced, alongside closures at a single point. We then present the characteristics of the mean velocity distribution and the

effects of the Reynolds number, analyzed in detail in [TAR 11a] and [TAR 11b]. Turbulence intensities of the velocity components are discussed in a separate section. The chapter ends with some reminders concerning vorticity, and its statistical characteristics in wall turbulent flows.

1.2. General equations

It will be assumed in this book that the readers are familiar with the basic concepts of fluid dynamics. Here, we will recap the basic equations applicable to fluid dynamics, limiting our examination to incompressible flows.

1.2.1. *Eulerian relations*

The two local equations that are fundamental in fluid dynamics express the conservation of mass and the first law of general mechanics, which results in the momentum balance equation. They are both expressed in terms of the material derivative[1] defined by

$$\frac{D}{Dt} = \frac{\partial}{\partial t} + U_i \frac{\partial}{\partial x_i} \qquad [1.1]$$

The component of the instantaneous local velocity vector in direction x_i is written as $U_i(\vec{x},t)$. The position vector is $\vec{x}(x_1,x_2,x_3)$ and t is the time. The Einstein summation notation is applied to the above relation. The material derivative expresses the variation of a physical value, tracking the particle in the flow.

1 The material derivative can also be spoken of as the particle derivative or Lagrangian derivative.

1.2.1.1. *Continuity equation*

The continuity equation expresses the conservation of mass throughout an elementary volume of fluid. It can be written in various forms, including

$$\frac{\partial \rho}{\partial t} + \frac{\partial \rho U_i}{\partial x_i} = 0 \qquad [1.2]$$

where ρ is the density. This equation can also be written as

$$\frac{D\rho}{Dt} + \rho \frac{\partial U_i}{\partial x_i} = 0 \qquad [1.3]$$

using the definition of the material derivative. In the context of the applications envisaged in this book, the density ρ is considered to be constant in this equation; so the continuity equation is reduced to

$$\frac{\partial U_i}{\partial x_i} = 0 \qquad [1.4]$$

1.2.1.2. *Momentum balance equations*

We obtain the momentum balance equations by applying Newton's first law to an elementary volume. We obtain

$$\frac{D\rho U_i}{Dt} = \frac{\partial}{\partial x_j}\sigma_{ji} + f_{ext,i} \qquad [1.5]$$

In this relation, $f_{ext,i}$ represents the external forces and σ_{ji} is the shear stress tensor defined by

$$\sigma_{ji} = -P\delta_{ji} + \mu D_{ji} - \frac{2\mu}{3}\left(\frac{\partial U_j}{\partial x_j}\right)\delta_{ji} \qquad [1.6]$$

for a Newtonian fluid.[2] In this equation, $P(\vec{x},t)$ represents the field of local instantaneous pressure, μ is the dynamic viscosity and δ_{ji} is the Kronecker delta ($\delta_{ji}=1$ if $j=i$, and 0 if not). The value D_{ij} is the strain tensor, which is expressed by

$$D_{ji}=\frac{\partial U_j}{\partial x_i}+\frac{\partial U_i}{\partial x_j} \qquad [1.7]$$

The momentum balance equation [1.4] can be reduced to the NS equation for an incompressible Newtonian fluid with constant viscosity. The NS equation is written, in tensor form, as

$$\frac{DU_i}{Dt}=\frac{\partial U_i}{\partial t}+U_j\frac{\partial U_i}{\partial x_j}=-\frac{1}{\rho}\frac{\partial P}{\partial x_i}+\nu\frac{\partial^2 U_i}{\partial x_j\partial x_j}+\frac{1}{\rho}f_{ext,i} \qquad [1.8]$$

where $\nu=\mu/\rho$ is the kinematic viscosity. A slightly different form of the NS equation is

$$\frac{\partial U_i}{\partial t}+\frac{\partial U_iU_j}{\partial x_j}=-\frac{1}{\rho}\frac{\partial P}{\partial x_i}+\nu\nabla^2 U_i+\frac{1}{\rho}f_{ext,i} \qquad [1.9]$$

As a general rule, the Einstein summation over repeated indices is adopted in this book, except in certain very specific cases, which will be clearly indicated. The viscous terms are contained in the Laplacian operator $\nabla^2=\partial^2/\partial x_j\,\partial x_j$ in equation [1.9].

2 The discussion in this book is strictly limited to incompressible flows of Newtonian fluids.

1.3. Notations

The complexity of certain equations means that we have to use the mixed forms of notation in this book. Figure 1.1 shows the notations that will be used. The position along the primary direction of the flow will be indicated by x or x_1. The instantaneous local velocity in this direction will be denoted either by U or by U_1 depending on the context. We will denote the component in the wall-normal direction y (or x_2) by V or U_2. The spanwise direction will be indicated by z (or x_3) with the corresponding velocity component written as W or U_3.

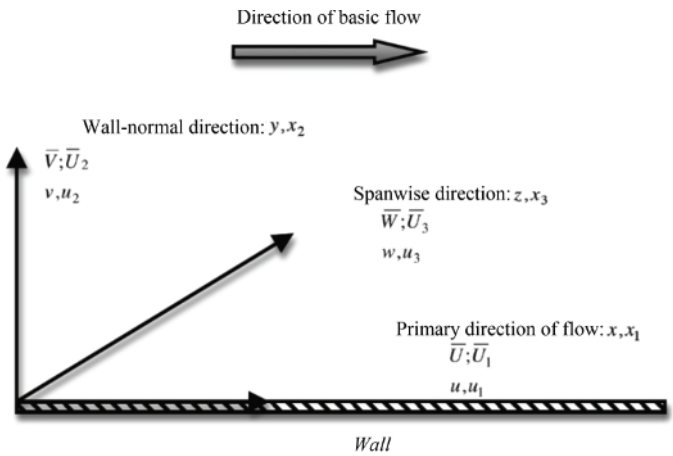

Figure 1.1. *Notations*

1.4. Reynolds equations

Consider the equation of *instantaneous* momentum along, say, the direction x for an incompressible fluid:

$$\frac{\partial U}{\partial t} + \frac{\partial U^2}{\partial x} + \frac{\partial UV}{\partial y} + \frac{\partial UW}{\partial z} = -\frac{1}{\rho}\frac{\partial P}{\partial x} + \nu \nabla^2 U \qquad [1.10]$$

where U, V and W are, respectively, the instantaneous components of the velocity vector in directions x, y and z, and P is the (instantaneous) pressure. The final term includes all the viscosity terms. This equation is valid at any time t (with the appropriate initial and boundary conditions). The instantaneous components of the velocity vector $U_i = U_i(\vec{x},t)$ vary in time and space, while the flow, at any given time, is highly unsteady and three-dimensional (3D). If we look at the behavior of $\vec{u}$ over long periods, then we need to average equation [1.10] over time. To do so, we decompose each physical value $Q(\vec{x},t)$ into a temporal average value $\overline{Q}(\vec{x})$ and a fluctuating value $q(\vec{x},t)$, where $\overline{q} = 0$. Thus we have, for example, $\overline{U_i U_j} = \overline{(\overline{U}_i + u_i)(\overline{U}_j + u_j)} = \overline{U}_i \overline{U}_j + \overline{u_i u_j}$, and the correlation between the fluctuations $\overline{u_i u_j}$ is generally non-null. Equation [1.10], subjected to this treatment and appropriately arranged, is written as

$$\overline{U}\frac{\partial \overline{U}}{\partial x} + \overline{V}\frac{\partial \overline{U}}{\partial y} + \overline{W}\frac{\partial \overline{U}}{\partial z} = -\frac{1}{\rho}\frac{\partial \overline{P}}{\partial x} + \nu \nabla^2 \overline{U} - \frac{\partial \overline{uu}}{\partial x} - \frac{\partial \overline{uv}}{\partial y} - \frac{\partial \overline{uw}}{\partial z} \quad [1.11]$$

and generally:

$$\overline{U}_j \frac{\partial \overline{U_i}}{\partial x_j} = -\frac{1}{\rho}\frac{\partial \overline{P}}{\partial x_i} + \nu \nabla^2 \overline{U}_i - \frac{\partial \overline{u_i u_j}}{\partial x_j} \quad [1.12]$$

The continuity equation, for its part, is of the same form for the average field and the fluctuating field; in other words, $\partial \overline{U}_i / \partial x_i = 0$ and $\partial u_i / \partial x_i = 0$, with the latter identity being valid instantaneously. What we need to take away from these equations (and by comparison with a laminar flow) is the existence of the terms of inter-correlation or cross-correlation of the type $\overline{u_i u_j}$. These terms, called Reynolds

stress (which, more specifically, are $-\rho\overline{u_i u_j}$), introduce six unknowns, for which, *a priori*, we have no additional equations. The only possibility, then, is to link them to the shearing terms $\partial\bar{U}_i/\partial x_j$ by way of considerations that are usually phenomenological. The issue of turbulent flows in general, and wall turbulence in particular, lies precisely in the modeling of these terms, which enables us to *close* the system of equations.

1.5. Exact relations in a fully developed turbulent channel flow

We will now lay out a few exact solutions in the case of a fully developed 2D turbulent channel flow. These solutions will enable us to link the wall shear stress to the distribution of the Reynolds stresses and clearly establish the reason why turbulence increases transfers at the wall. The flow is homogeneous along the streamwise x and spanwise z directions, which gives us $\partial/\partial x = \partial/\partial z = 0$. The channel is considered to be infinite. Consequently, the spanwise velocity is $\bar{W} = 0$. For reasons of continuity, $\bar{V} = 0$ and $\bar{U} = \bar{U}(y)$. The Reynolds equations along the streamwise and wall-normal directions then assume the exact forms:

$$\begin{aligned} 0 &= -\frac{1}{\rho}\frac{\partial \bar{P}}{\partial x} + \nu\frac{\partial^2 \bar{U}}{\partial y^2} - \frac{\partial \overline{uv}}{\partial y} \\ 0 &= -\frac{1}{\rho}\frac{\partial \bar{P}}{\partial y} - \frac{\partial \overline{vv}}{\partial y} \end{aligned} \qquad [1.13]$$

We can see, from this last equation, that the pressure is not solely a function of x, but rather there are variations along y, induced by the gradient of $\overline{vv}$. This is the first difference from a laminar Poiseuille flow. Integration of

equation [1.53], from the wall ($y=0$) to a point of ordinate y in the flow, enables us to write

$$\frac{1}{\rho}\int_0^y \frac{\partial \overline{P}}{\partial y}dy = -\int_0^y \frac{\partial \overline{vv}}{\partial y}dy = -\overline{vv}(y)$$

such that $\overline{P}(x,y) = -\rho\overline{vv}(y) + \overline{P}_0(x)$, where $\overline{P}_0(x)$ is the pressure at the wall. Thus, $\frac{\partial \overline{P}}{\partial x} = \frac{d\overline{P}_0}{dx}$ for reasons of homogeneity ($\overline{vv}$ depends only on y).

We can then integrate the Reynolds equation relating to $\overline{U}(y)$, from the wall to the center of the channel ($y=h$), noting that the shear $\left(\partial\overline{U}/\partial y\right)_{y=h} = 0$ because of symmetry. We obtain

$$0 = -\frac{1}{\rho}\frac{d\overline{P}_0}{dx}h - \frac{1}{\rho}\overline{\tau}_0$$

because the Reynolds shear stress $-\rho\overline{uv}$ is null at the wall and in the center of the channel, again for reasons of symmetry. This last equation links the pressure gradient $d\overline{P}_0/dx$ to the friction at the wall $\overline{\tau}_0 = \mu\left(\partial\overline{U}/\partial y\right)_{y=0}$. By putting this value back into the equation of $\overline{U}$ and integrating it this time from the wall to y in the flow, we obtain

$$\mu\frac{\partial \overline{U}}{\partial y}(y) - \rho\overline{uv}(y) = \overline{\tau}_0\left(1 - \frac{y}{h}\right)$$

where on the left, we can clearly see the total shear stress

$$\overline{\tau}_{tot} = \mu\frac{\partial \overline{U}}{\partial y}(y) - \rho\overline{uv}(y) \qquad [1.14]$$

which is the sum of the viscous stress and the Reynolds stress. We introduce the friction velocity $\overline{u}_\tau$

$$\rho \overline{u}_\tau^2 = \overline{\tau}_0 \qquad [1.15]$$

and the internal length scale

$$l_\nu = \frac{\nu}{\overline{u}_\tau} \qquad [1.16]$$

The values rendered dimensionless by the wall units $\overline{u}_\tau$ and l_ν are indicated by $(\,)^+$. The dimensionless form of equation [1.14] in inner variables is

$$\overline{\tau}_{tot}^+ = \frac{\partial \overline{U}^+}{\partial y^+} - \overline{uv}^+ = 1 - \frac{y^+}{h^+} \qquad [1.17]$$

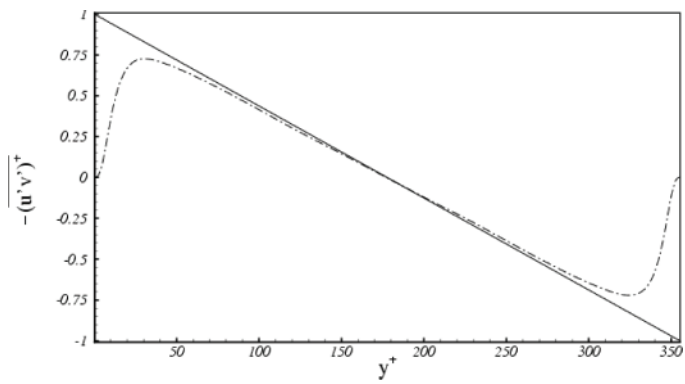

Figure 1.2. *Reynolds stress in wall units as a function of the distance to the wall. The solid line represents the total stress. These results are obtained on the basis of direct numerical simulations in a fully developed turbulent channel flow for* $Re_\tau = \frac{h\overline{u}_\tau}{\nu} = 180$. *(From [DOC 06])*

Thus, the total stress varies linearly with the distance from the wall. Relation [1.17] is exact. Figure 1.2 shows the

distributions of the Reynolds stress $-\overline{uv}^{+}$ and the total stress $\overline{\tau}_{tot}^{+}$ obtained by direct numerical simulations (DNSs) in a fully developed turbulent channel flow at a low Reynolds number. The results demonstrate perfect linearity of $\overline{\tau}_{tot}^{+}$, and this type of analysis enables us to check the quality of the results (such as the statistical convergence, for example), both experimental and numerical. DNSs resolve the integrality of the scales defined by discretization of the domain of calculation, and of course, do not require closure. We can go one step further and also determine the friction coefficient. Integration of equation [1.17], from the lower wall of the channel to y^{+} in the flow, gives us the velocity distribution.

$$\overline{U}^{+}\left(y^{+}\right)=y^{+}-\frac{y^{+2}}{2h^{+}}+\int_{0}^{y^{+}}\overline{uv}^{+}\left(\eta^{+}\right)d\eta^{+} \qquad [1.18]$$

By integrating this relation from the wall to the center ($y^{+}=h^{+}$), we arrive at:

$$\int_{0}^{h^{+}}\overline{U}^{+}\left(y^{+}\right)dy^{+}=\frac{h^{+2}}{3}+\int_{0}^{h^{+}}\left[\int_{0}^{y^{+}}\overline{uv}^{+}\left(\eta^{+}\right)d\eta^{+}\right]dy^{+}$$

The latter integral can be calculated by integration by parts:

$$\int_{0}^{h^{+}}\left[\int_{0}^{y^{+}}\overline{uv}^{+}\left(\eta^{+}\right)d\eta^{+}\right]dy^{+}=\int_{0}^{h^{+}}\left(h^{+}-y^{+}\right)\overline{uv}^{+}\left(y^{+}\right)dy^{+}$$

Using the definition of the bulk velocity $\overline{U}_{m}^{+}=\frac{1}{h^{+}}\int_{0}^{h^{+}}\overline{U}^{+}\left(y^{+}\right)dy^{+}$, we find:

$$\overline{U}_m^+ = \frac{h^+}{3} - \int_0^{h^+} \left(1 - \frac{y^+}{h^+}\right)\left(-\overline{uv}^+\right) dy^+$$

It is interesting to rewrite this equation using the scales h and $\overline{U}_m$, known as "external (outer) scales", to find a relation concerning the friction coefficient, here defined by $C_f = \overline{\tau}_p / 1/2\rho\overline{U}_m^2 = 2/\overline{U}_m^{+2}$. By introducing $Re = \overline{U}_m h/\nu$, noting that $h^+ = Re_\tau = h\overline{u}_\tau/\nu = Re/\overline{U}_m^+$, and using the notation $(\ )^*$ to represent the values rendered dimensionless by h and $\overline{U}_m$, we obtain:

$$C_f = \frac{6}{Re} + 6\int_0^1 \left(1 - y^*\right)\left(-\overline{uv}^*\right) dy^* \qquad [1.19]$$

The quantity $6/Re$ is nothing but the friction coefficient for a laminar flow. It can be interpreted as the laminar contribution C_{fl} in this specific case. The second term on the right of the previous equation is a weighted integral of the distribution of the Reynolds stresses and constitutes the direct contribution of the turbulence to the friction coefficient, written as C_{ft}. The turbulence considerably increases the friction coefficient, because of this contribution. Equation [1.19] was also obtained, in a slightly different manner, by [FUK 02].

We can go further with the analysis and see whether it is possible to decompose the velocity field into laminar and turbulent contributions. Equation [1.18] used with the external scales h and $\overline{U}_m$ is

$$\overline{U}^*\left(y^*\right)=\frac{Re}{2}C_f\left(y^*-\frac{y^{*2}}{2}\right)+\int_0^{y^*}\overline{uv}^*\left(\eta^*\right)d\eta^*$$

We propose the decomposition $\overline{U}^*=\overline{U}_l^*+\overline{U}_t^*$, where, for a given Re ($\overline{U}_m$), $\overline{U}_l^*=3/2\,y^*\left(2-y^*\right)$ is the laminar (Poiseuille) velocity profile and $\overline{U}_t^*$ is the turbulent contribution to $\overline{U}^*$, which remains to be determined. By decomposing $C_f=C_{fl}+C_{ft}$ in equation [1.19] and after arrangement, we obtain:

$$\overline{U}_t^*=\frac{3Re}{2}y^*\left(2-y^*\right)\left\{\int_0^1\left(1-y^*\right)\left(-\overline{uv}^*\right)dy^*-\int_0^{y^*}-\overline{uv}^*\left(\eta^*\right)d\eta^*\right\} \quad [1.20]$$

in the absence of Reynolds stresses, obviously, $\overline{U}_t^*$ becomes null.

1.6. Equations for a turbulent boundary layer

Consider a 2D turbulent boundary layer. The Reynolds equations for an incompressible fluid with constant physical properties are:

$$\begin{aligned}\overline{U}\frac{\partial\overline{U}}{\partial x}+\overline{V}\frac{\partial\overline{U}}{\partial y}&=-\frac{1}{\rho}\frac{\partial\overline{P}}{\partial x}+\nu\left[\frac{\partial^2\overline{U}}{\partial x^2}+\frac{\partial^2\overline{U}}{\partial y^2}\right]-\frac{\partial\overline{uu}}{\partial x}-\frac{\partial\overline{uv}}{\partial y}\\ \overline{U}\frac{\partial\overline{V}}{\partial x}+\overline{V}\frac{\partial\overline{V}}{\partial y}&=-\frac{1}{\rho}\frac{\partial\overline{P}}{\partial y}+\nu\left[\frac{\partial^2\overline{V}}{\partial x^2}+\frac{\partial^2\overline{V}}{\partial y^2}\right]-\frac{\partial\overline{uv}}{\partial x}-\frac{\partial\overline{vv}}{\partial y}\end{aligned} \quad [1.21]$$

The terms in $\partial/\partial z$ disappear because the turbulent flow is 2D (in the case of a boundary layer on a flat plate, for example, its spanwise extent is assumed to be infinite). The last terms in these equations represent the contributions of fluxes of turbulent shear stresses. The boundary layer

approximations, which we are about to develop, are based on an important peculiarity concerning the order of magnitude of u, v and w. The continuity equation for the fluctuating components is written thus:

$$\frac{\partial u}{\partial x}+\frac{\partial v}{\partial y}+\frac{\partial w}{\partial z}=0$$

However, a structure responsible for turbulent fluctuations has no prevailing direction (in a rough sense), and its characteristic scales in the three directions are, locally, of the same order of magnitude

$$l_x \cong l_y \cong l_z = \ell$$

The symbol $\cong$ needs to be interpreted as being *of the order of* rather than *approximately equal to*. The continuity equation thus implies

$$u' \cong v' \cong w' = u'$$

(Figure 1.3). The order of magnitude of the fluctuations is, therefore, estimated by

$$\frac{\partial \overline{u'u'}}{\partial x} \cong \frac{u'^2}{\mathcal{L}} << \frac{\partial \overline{u'v'}}{\partial y} \cong \frac{u'^2}{\overline{\delta}}$$

because $\overline{\delta} << \mathcal{L}$. It follows that

$$\frac{\partial^2 \overline{U}}{\partial x^2} << \frac{\partial^2 \overline{U}}{\partial y^2}$$

$$\frac{\partial \overline{P}}{\partial y} << \frac{\partial \overline{P}}{\partial x} \Rightarrow \overline{P} = \overline{P}_\infty(x)$$

$$-\frac{1}{\rho}\frac{d\overline{P}_\infty}{dx} = \overline{U}_\infty \frac{d\overline{U}_\infty}{dx}$$

The turbulent boundary layer equations are finally reduced to:

$$\bar{U}\frac{\partial \bar{U}}{\partial x}+\bar{V}\frac{\partial \bar{U}}{\partial y}=\bar{U}_{\infty}\frac{d\bar{U}_{\infty}}{dx}+\nu\frac{\partial^2 \bar{U}}{\partial y^2}-\frac{\partial \overline{uv}}{\partial y} \qquad [1.22]$$

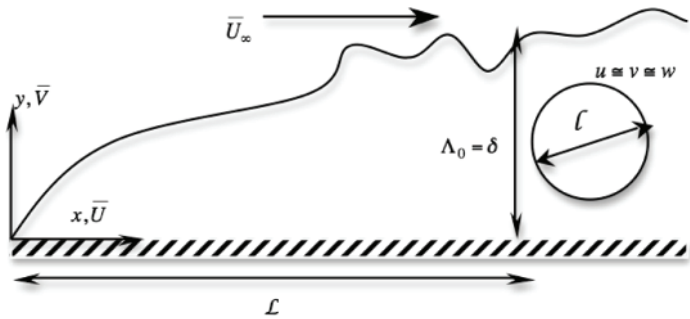

Figure 1.3. *Scale characteristics of a turbulent boundary layer and a local turbulent structure*

1.7. Scales in a wall-bounded turbulent flow

We will begin by introducing the velocity and length scales needed to describe the physics of wall turbulence and turbulent transfer at the rigid boundary. The meaning of these scales will become clearer when we introduce the mixing-length-type closures later in this chapter. Generally speaking, we can distinguish two zones in a wall flow: a near-wall zone, where the flow is controlled by the *internal scales*, and a zone relatively far from the wall, governed by the *external scales*.

The near-wall zone is characterized by the wall shear stress $\bar{\tau}_0 = \mu\left(\partial\bar{u}/\partial y\right)_0$ and the kinematic viscosity ν. We introduce a fictitious velocity $\bar{u}_\tau = \sqrt{\bar{\tau}_0/\rho}$ based on the shear at the wall, called the friction velocity. This velocity scale accurately describes the turbulent state near to the wall, because without shear (vorticity), no turbulence can be

sustained. The length scale based on the friction velocity and the viscosity is $l_\nu = \nu/\overline{u}_\tau$. The couple $(\overline{u}_\tau, l_\nu)$ constitutes the internal scales. The quantity q, rendered dimensionless by the internal scales, is denoted by q^+, such as, e.g. the velocity $\overline{U}^+ = \overline{U}/\overline{u}_\tau$, the Reynolds stress $-\overline{u_i u_j}^+ = -\overline{u_i u_j}/\overline{u}_\tau^2$, the time $t^+ = t\overline{u}_\tau^2/\nu$ or the frequency $f^+ = f\nu/\overline{u}_\tau^2$ in wall units. The internal scale is constant in the case of a turbulent flow in a channel, but it depends on the streamwise direction x in a turbulent boundary layer. Consequently, the adimensionalization by the wall scales $(\overline{u}_\tau(x), l_\nu)$ only makes sense for a given local position x in the latter case. Among other things, this requires that the turbulent boundary layer should be at equilibrium. The notion of turbulence at equilibrium is an important one, and one that is sometimes tricky to grasp. Interested readers can, for example, consult [TOW 76], which is one of the classic works in this domain.

The external velocity scale is either the velocity $\overline{U}_c$ in the center of the channel or its bulk velocity $\overline{U}_m$, or the velocity in the irrotational zone of a boundary layer $\overline{U}_\infty$. In parallel, the external length scale Λ_0 is the half-height of the channel h or the thickness of the turbulent boundary layer. The external scales are universal, unlike the internal scales, which are linked to the localized phenomenology, near to the wall.

1.8. Eddy viscosity closures

Consider the terms:

$$\nu\frac{\partial^2\overline{U}}{\partial y^2} - \frac{\partial\left(\overline{uv}\right)}{\partial y} = \frac{1}{\rho}\frac{\partial}{\partial y}\left(\mu\frac{\partial\overline{U}}{\partial y} - \rho\overline{uv}\right)$$

in the Reynolds equation. As previously indicated, and *a fortiori* in the above representation, it is clear that $-\rho\overline{uv}$ plays the physical role of a stress. The Reynolds stress is positive in a flow where the gradient $\partial\bar{U}/\partial y > 0$, and it increases the total stress.

Thus, the stress $-\rho\overline{uv}$ is added to the viscous stress to yield the total stress $\bar{\tau}_{tot}$. One typical way to model $-\rho\overline{uv}$ is to link it to the average gradient $\partial\bar{U}/\partial y$, because, without shear, no turbulence is produced. We then introduce a fictitious viscosity, $\nu_t(y)$, called the eddy (or turbulent) viscosity, and express the Reynolds stress as

$$-\overline{uv} = \nu_t(y)\frac{\partial\bar{U}}{\partial y} \qquad [1.23]$$

The eddy viscosity $\nu_t(y)$ is not strictly linked to vortices, although coherent vortex structures, particularly near to the wall, play an important part in generating turbulence. The turbulent viscosity is not a physical property of the fluid – far from it. It is not a constant, and varies spatially. There is no universal model for $\nu_t(y)$, and it depends on the phenomenology of the particular flow.

Thus, the total stress can be written as

$$\bar{\tau}_{tot} = \rho\left[\nu + \nu_t(y)\right]\frac{\partial\bar{U}}{\partial y}$$

Essentially, we can distinguish two zones in a wall layer, depending on whether the eddy viscosity is greater or lesser than the kinematic viscosity. The kinematic viscosity is predominant in a confined sublayer near to the wall, where

$\nu_t(y) << \nu$. We can expand the velocity $\bar{U}(y)$ into a Taylor series near to the wall:

$$\bar{U}(y) = \left(\frac{\partial \bar{U}}{\partial y}\right)_{y=0} y + \frac{1}{2}\left(\frac{\partial^2 \bar{U}}{\partial y^2}\right)_{y=0} y^2 + \frac{1}{6}\left(\frac{\partial^3 \bar{U}}{\partial y^3}\right)_{y=0} y^3 + \ldots.$$

and by virtue of how thin the sublayer is, we can neglect the terms of greater order than y:

$$\bar{U}(y) \approx \left(\frac{\partial \bar{u}}{\partial y}\right)_{y=0} y = \frac{\bar{\tau}_0}{\mu} y$$

Using the internal scales $(\nu, \bar{u}_\tau)$ introduced in section 1.7, we find:

$$\bar{U}^+\left(y^+\right) = y^+ \qquad [1.24]$$

in this layer commonly known as the viscous sublayer. The linearity of the velocity distribution in relation to the wall-normal distance is nothing out of the ordinary, and also, such a zone exists whether we are dealing with a laminar or a turbulent flow. The fact that the viscosity is predominant in this zone absolutely does not mean that the flow is laminar, and in fact the term "laminar sublayer" is utterly erroneous: the turbulent fluctuations are very strong in the viscous sublayer. For example, the turbulent intensity of the wall shear stress fluctuations $\sqrt{\overline{\tau'_0 \tau'_0}} \big/ \bar{\tau}_0$ is as high as 0.40.

Now let us consider the zone of flow, where the eddy viscosity is dominant, with $\nu_t >> \nu$. This zone, in which the viscous effects are negligible with respect to the effect of turbulent mixing, is relatively far from the wall. We suppose, however, that the total stress $\bar{\tau}_{tot}$ remains constant and is equal to the stress at the wall $\bar{\tau}_0$ (Figure 1.4). For this

reason, this layer is called the constant stress sublayer. With these hypotheses made, we can write:

$$\overline{\tau}_{tot} \equiv \overline{\tau}_0 = \rho \nu_t(y) \partial \overline{U} / \partial y$$

We still need to model the eddy viscosity $\nu_t(y)$. It can take the form $\nu_t(y) \approx \ell \nu$, where ℓ and ν are the length- and velocity scales characterizing the turbulent mixing. In relation to ν, the choice of the friction velocity $\overline{u}_\tau$ proves logical, given that the phenomenon, overall, is determined by the stress at the wall. The length scale typical of the turbulent viscosity is the wall-normal distance: the extent of the turbulent mixing increases with y and $\ell = \kappa y$, where κ is a constant. Closure in turbulent flows is generally based on phenomenology. Thus, the hypotheses made must be compared against the experimental results or the direct numerical simulations. There is no general rule that can be applied here. The closure $\ell = \kappa y$, where κ is the universal von Kárman coefficient, was one of the earliest propositions to be made.

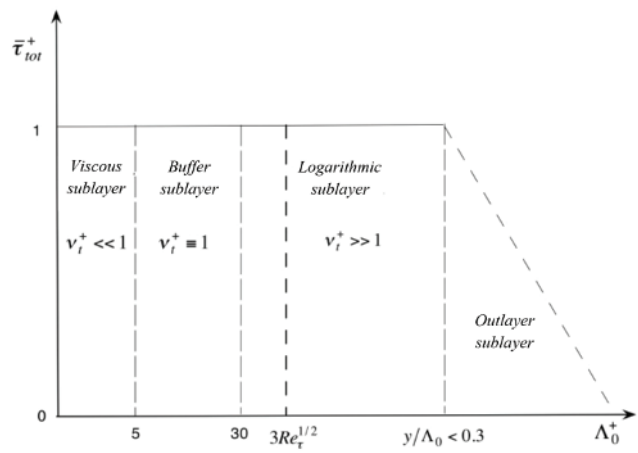

Figure 1.4. *Sublayers in a turbulent wall flow*

By expressing these different hypotheses using internal scales (in particular, $\nu_t^+ = \nu_t / \nu$) we conclude:

$$\overline{\tau}_{tot}^+ = 1 = \nu_t^+ \left(y^+ \right) \frac{d\overline{U}^+}{dy^+} = \kappa y^+ \frac{d\overline{U}^+}{dy^+}$$

and by integrating this expression, we find a logarithmic velocity distribution:

$$\overline{U}^+ \left(y^+ \right) = \frac{1}{\kappa} \ln y^+ + B \qquad [1.25]$$

The constant B does not depend greatly on the Reynolds number, and varies between $B = 4.5$ and $B = 5.5$. The von Kárman constant, within the limit of large Reynolds numbers, is $\kappa = 0.37$, as is also predicted by the renormalization group theory [TAR 11a, TAR 11b]. The zone of overlap between the viscous sublayer and logarithmic sublayer is called the buffer sublayer. It plays a dynamic role which is crucially important in wall turbulence. The so-called coherent vortex structures are concentrated mainly in this zone. The coherent vortices, to which this book is entirely dedicated, are responsible for the regeneration of the Reynolds stresses and the turbulent mixing. A semi-empirical expression for the velocity distribution, which corresponds well to the measurements, particularly in the lower buffer sublayer, is

$$\overline{u}^+ \left(y^+ \right) = 14.5 \tanh \left(\frac{y^+}{14.5} \right) \qquad [1.26]$$

This expression is based on [RAN 56][3], which suggests

$$\nu_t^+ = \sinh^2 \left(\chi y^+ \right)$$

3 See [HIN 75, p. 622].

in the viscous- and buffer sublayers, and the empirical value of χ is $\chi = 14.5$. The validity of this expression in wall turbulence with very large Reynolds numbers has not been established.

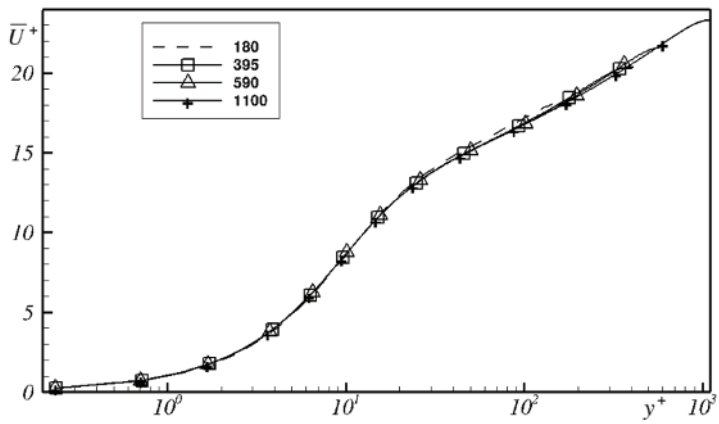

Figure 1.5. *Mean velocity profiles in a fully developed turbulent channel flow. The results were obtained by Bauer [BAU 14] using direct numerical simulations in the range* $Re_\tau = 180$ *to* $Re_\tau = 1{,}100$

The mean velocity is a value, which is relatively simple to measure, and there is a huge database of experimental readings taken of $\overline{U}^+\left(y^+\right)$. By way of illustration, in Figure 1.5, we show the mean velocity profiles obtained by direct numerical simulations[4] in a fully developed turbulent

4 We present our own direct numerical simulations for illustrative purposes. Larger Reynolds numbers have now been attained in channels and boundary layers, in wide domains of calculation up to $Re_\tau = 2{,}000$ [HOY 08] and turbulent boundary layers with $Re_\tau = 1{,}271$ in [SCH 10] and $Re_\tau = 2{,}000$ in [SIL 11]. These limits increase as our computational capacities increase. Readers can usefully consult http://www.mech.kth.se/~pschlatt/DATA/, and http://torroja.dmt.upm.es/channels/data/. At present, J. Jiménez and R. Mosser are working on direct numerical simulations in a pipe with $Re_\tau = 5{,}000$.

channel flow covering a range from small Reynolds numbers $Re_\tau = \overline{u}_\tau h / \nu = 180$ to moderate values $Re_\tau = 1{,}100$. Indeed, we can see a sublayer wherein $\overline{U}^+ \propto \ln\left(y^+\right)$ which, apparently, begins at $y^+ = 30$. A more detailed analysis, though, reveals that the von Kárman constant κ has not yet reached its asymptotic value, because the Reynolds numbers in question here are small, and the "logarithmic layer" is not entirely free of viscous effects in the case shown in Figure 1.5. Let us stress the highly restrictive nature of the numerous hypotheses that have led us to relation [1.25], which, in particular, requires that the viscous stress be negligible and the Reynolds stress $-\overline{uv}^+$ be constant and equal to 1 in that zone. However, rigorously speaking, these hypotheses are valid only within the range $Re_\tau \to \infty$. Thus, in the range of Re_τ values considered here, the zone wherein the Reynolds stress is constant and "approximately" equal to the stress at the wall (though not exactly equal) is greatly restricted, as shown by Figure 1.6.

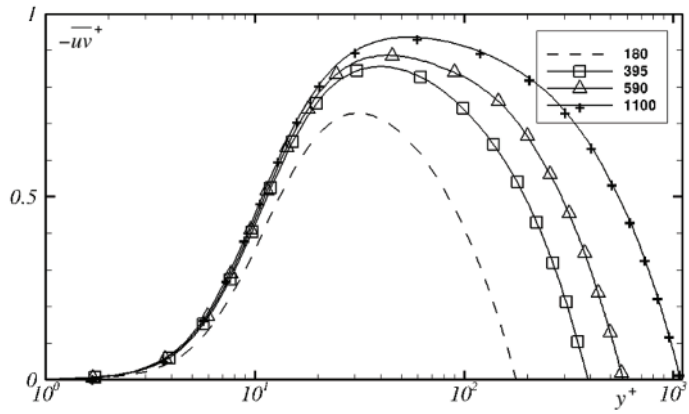

Figure 1.6. *Profiles of the Reynolds stress in units wall in a fully developed turbulent channel flow. The results are obtained by Bauer [BAU 14] by direct numerical simulations in the range* $Re_\tau = 180$ *to* $Re_\tau = 1{,}100$

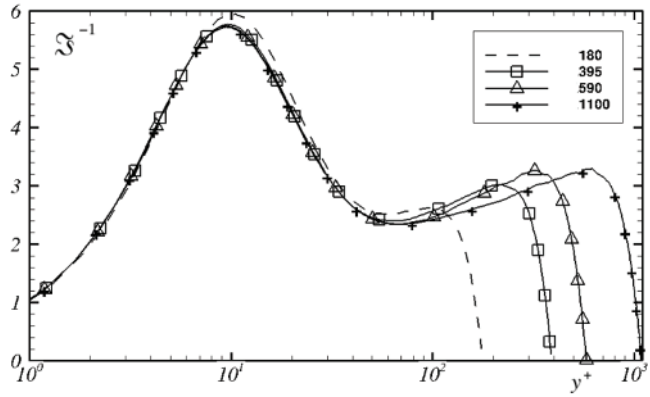

Figure 1.7. *Inverse of the "diagnostic" function depending on the distance to the wall in a turbulent channel flow using direct numerical simulations, taken from [BAU 14]*

Consider the so-called "diagnostic" function

$$\Im = \left(y^+ \frac{d\overline{U}^+}{dy^+} \right)^{-1} \qquad [1.27]$$

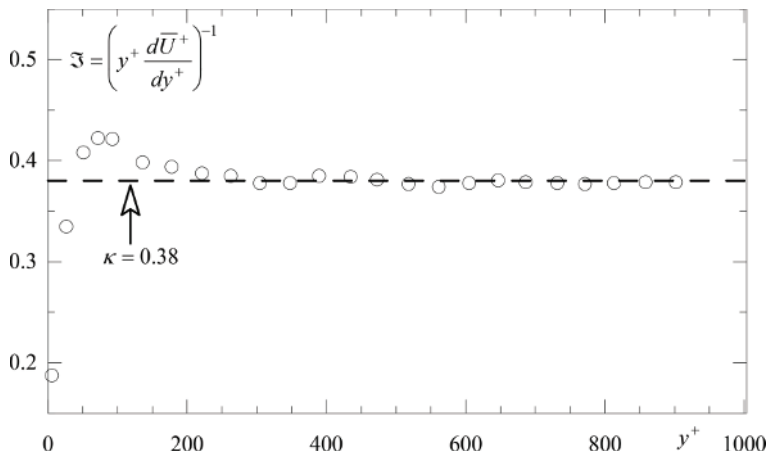

Figure 1.8. *"Diagnostic" function based on the wall-normal distance in wall scales, according to [OST 00]. The data are averaged over different profiles in the inner layer* $y/\delta < 0.15$, *where* δ *is the thickness of the boundary layer*

This quantity can be reduced to the von Kármán constant, $\Im = \kappa$, which should be independent of the Reynolds number in a *universal* logarithmic sublayer.[5] Figure 1.7 shows the distributions of $\Im^{-1}(y^+)$ found by direct numerical simulation by Bauer [BAU 14]. Note the emergence of a zone beginning at approximately $y^+ = 50$ in which $\Im^{-1}(y^+)$ varies little but does not remain perfectly constant. The size of this zone increases with increasing Re_τ, as might be expected.

Let us attempt to clarify the situation by analyzing Figure 1.8, which shows the distribution of $\Im\left(y^+\right)$ on the basis of the wall-normal distance in inner units. The figure is adapted from [OST 00], and includes the experimental data on the boundary layer in a wide range of Reynolds number values, based on the momentum thickness covering $2{,}500 \leq Re_\theta \leq 27{,}000$. We note that $\Im = \kappa$ does indeed tend toward a universal value independent of the Reynolds number, but quite far from the wall at $y^+ \geq 200$ (the data are averages over different profiles with different Re values). Although they are slight, the viscous effects extend from the end of the buffer sublayer $y^+ = 30$ to $y^+ = 200$, depending on the Reynolds number. A *universal logarithmic* sublayer of significant extent would, therefore, exist only beyond $y^+ = 200$, and then only if the Reynolds number is sufficiently high – typically $Re_\theta \geq 6{,}000$.[6] The logarithmic zone would not be entirely free of viscous effects at $Re_\theta \leq 6{,}000$, and the von Kármán constant would depend on the Reynolds number, as shown in [OST 00] and Figure 1.8.

---

5 Readers can consult [TAR 11a] and [TAR 11b], and the references cited therein, for a detailed discussion of the state of the art on the structure of the mean velocity distribution in different sublayers. In this chapter, we content ourselves with a very restricted overview.

6 Using the semi-empirical relation $\delta^+ = Re_\tau = 0.30\, Re_\theta$ from [GEO 97], we obtain the limit $Re_\tau > 1{,}800$.

Figure 1.9 shows the von Kármán constant deduced from the measurements taken by Osterlund *et al.* [OST 00] and Nagib and Hites [NAG 95]. The maximum Reynolds number attained in these experiments is approximately $Re_\theta = 28\times10^3$. The von Kármán constant was determined in the inner layer delimited by $50 \le y^+ \le 0.15\delta^+$. We have expressed κ as the value predicted by the renormalization group $\kappa_{RNG} = 0.37$, and represent the data as a function of $1/\ln Re_\theta$. In spite of an inherent dispersion, we note that the von Kármán constant increases with $1/\ln Re_\theta$. A linear regression suggests the variation $\kappa/\kappa_{RNG} \propto 5/\ln Re_\theta$. According to the results presented in

Figure 1.9, the von Kármán constant reaches its value $\kappa_{RNG} = 0.37$ at $Re_\theta = 50\times10^3$ – a limit beyond which it should, in theory, remain constant.

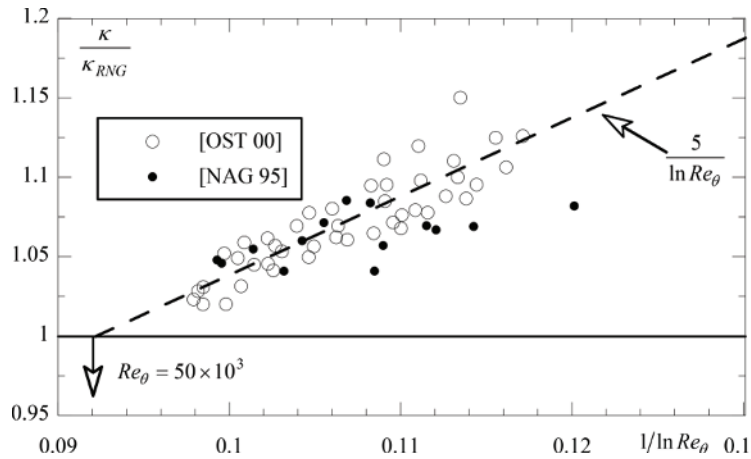

Figure 1.9. *The von Kármán constant expressed as its value obtained by the renormalization group as a function of the Reynolds number. Experimental data harvested from [OST 00] and [NAG 95]. This figure is adapted from [TAR 11b]*

The logarithmic sublayer in the "universal" sense of the term would thus exist only when $Re_\tau > 1800$. Recent research has shown that it begins at $y^+ \equiv 3\sqrt{Re_\tau}$ [KLE 09, ALF 11, MAR 13] within the range of moderate Reynolds numbers (Figure 1.4), and ends at approximately $y/\Lambda_0 = 0.15$, where, remember, Λ_0 is the integral scale (the half-height of the channel, or the thickness of the boundary layer). The outer limit in internal scales is clearly $0.15Re_\tau$ [MAR 13]. The von Kárman constant determined by analysis of experimental data by Marusic *et al.* [MAR 13] is $\kappa = 0.39$ in the range $18\times10^3 < Re_\tau < 63\times10^4$, which differs only very slightly from the value *RNG* $\kappa_{RNG} = 0.37$.[7] Regarding the constant B in the logarithmic distribution [1.25], its value is $B = 4.3$.

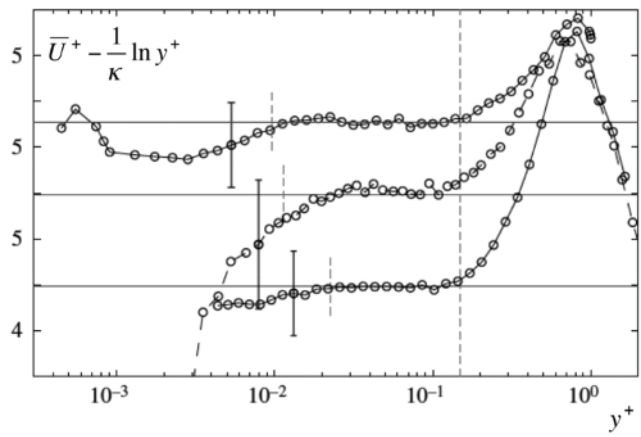

Figure 1.10. *The profiles* $\overline{U}^+ - (1/\kappa)\ln y^+$ *according to [MAR 13]. Top to bottom:* $Re_\tau = 98{,}190$*, 68,780 and 18,010. The vertical dotted lines delimit the zone* $3\sqrt{Re_\tau} \le y^+ \le 0.15Re_\tau$*. The experimental error bands are also shown in the figure*

7 It is interesting to note that the lowest Reynolds number used in Marusic's study corresponding to $Re_\tau = 18\times10^3$ is approximately $Re_\theta = 60\times10^3$. The von Karman constant must, therefore, have reached its asymptotic value of *RNG*, in light of Figure 1.9, which is perfectly the case.

Figure 1.10, adapted from [MAR 13], shows three experimental profiles $\bar{U}^+ - (1/\kappa)\ln y^+$, where $\kappa = 0.39$, in the range $98{,}190 \le Re_\tau \le 18{,}010$. We can see that the profiles do indeed reach plateau regions in the zone $3\sqrt{Re_\tau} \le y^+ \le 0.15 Re_\tau$.

The velocity in the outer sublayer depends on the friction velocity $\bar{u}_\tau$, the velocity $\bar{U}_\infty$ in the potential zone of a boundary layer (or the velocity at the center of the channel $\bar{U}_c$), the distance y from the wall and the external length scale Λ_0 (the thickness δ of the boundary layer or the half-height h of channel). A simple similarity analysis shows that $\bar{U}(y)$ is of the form:

$$\frac{\bar{U}_\infty - \bar{U}(y)}{\bar{u}_\tau} = \bar{U}_\infty^+ - \bar{U}^+\left(y^+\right) = g\left(\frac{y}{\Lambda_0}\right) \qquad [1.28]$$

in that zone. More generally, and taking account of $\bar{u}_\tau / \bar{U}_\infty$, we can write

$$\frac{\bar{U}_\infty - \bar{U}(y)}{\bar{u}_\tau} = \bar{U}_\infty^+ - \bar{U}^+\left(y^+\right) = g\left(\frac{y}{\Lambda_0}, \frac{\bar{u}_\tau}{\bar{U}_\infty}\right) \qquad [1.29]$$

The introduction of the Rotta thickness [ROT 50]

$$\delta_R = \int_0^\infty \frac{\bar{U}_\infty - \bar{U}(y)}{\bar{u}_\tau} dy \qquad [1.30]$$

enables us to express the velocity defect distribution as

$$\frac{\bar{U}_\infty - \bar{U}(y)}{\bar{u}_\tau} = \bar{U}_\infty^+ - \bar{U}^+\left(y^+\right) = g\left(\frac{y}{\delta_R}\right) \qquad [1.31]$$

with the function g from equation [1.29] repeated here for ease of notation.

The Rotta thickness is linked to the displacement thickness δ_d by

$$\begin{aligned}\delta_R(x) &= \int_0^\infty \frac{\bar{U}_\infty - \bar{U}(y)}{\bar{u}_\tau} dy = \int_0^\infty \frac{\bar{U}_\infty - \bar{U}(y)}{\bar{U}_\infty} \frac{\bar{U}_\infty(x)}{\bar{u}_\tau(x)} dy \\ &= \delta_d(x) \frac{\bar{U}_\infty(x)}{\bar{u}_\tau(x)}\end{aligned} \quad [1.32]$$

where it must be remembered that x and y are, respectively, the coordinates in the streamwise and wall-normal directions. Equation [1.32] is also written as

$$\delta_d(x) = \delta_R(x) \left(\frac{\bar{U}_\infty(x)}{\bar{u}_\tau(x)} \right)^{-1} = \delta_R(x) \left(\bar{U}_\infty^+ \right)^{-1} \quad [1.33]$$

By introducing the outer variable $\eta = y/\delta_R$, it is easy to verify that the definition of the Rotta thickness yields

$$\int_0^\infty g(\eta) d\eta = 1 \quad [1.34]$$

It is also possible to determine a simple relation concerning the form factor $H(x) = \delta_d(x)/\theta(x)$. Indeed

$$\theta(x) = \int_0^\infty \frac{\bar{U}(y)}{\bar{U}_\infty} \left(\frac{\bar{U}_\infty - \bar{U}(y)}{\bar{U}_\infty} \right) dy = \delta_R(x) \left(\bar{U}_\infty^+ \right)^{-1} \int_0^\infty \left(1 - \left(U_\infty^+ \right)^{-1} g(\eta) \right) g(\eta) \, d\eta$$

which, in light of equation [1.34], is reduced to

$$\theta(x) = \delta_R(x) \left(\bar{U}_\infty^+ \right)^{-1} - \delta_R(x) \left(\bar{U}_\infty^+ \right)^{-2} \int_0^\infty g^2(\eta) d\eta \quad [1.35]$$

Hence, the shape factor is

$$H(x)=\frac{1}{1-\left(\bar{U}_{\infty}^{+}\right)^{-1}\int_{0}^{\infty}g^{2}(\eta)d\eta} \qquad [1.36]$$

The linking of the profiles in the inner and outer layers results in an intermediate logarithmic distribution. In the internal layer, the velocity is governed by a function that depends on the wall variables, so that

$$\bar{U}\left(y^{+}\right)=\bar{u}_{\tau}f\left(\frac{y\bar{u}_{\tau}}{\nu}\right) \qquad [1.37]$$

This profile needs to be linked to the outer profile, described by equation [1.28] in the intermediate layer. We have:

$$\bar{U}_{\infty}-\bar{U}(y)=\bar{U}_{\infty}-\bar{u}_{\tau}f\left(\frac{y\bar{u}_{\tau}}{\nu}\right)=\bar{u}_{\tau}g\left(\frac{y}{\Lambda_{0}}\right) \qquad [1.38]$$

at the overlap point. The derivative in relation to y in the above equation enables us to write:

$$\frac{\bar{u}_{\tau}}{\nu}f'\left(y^{+}\right)=-\frac{1}{\Lambda_{0}}g'\left(\frac{y}{\Lambda_{0}}\right)=-\frac{1}{\Lambda_{0}}g'(\eta)$$

where $\eta=y/\Lambda_{0}$. By multiplying both sides of the above equation by y, we obtain:

$$y^{+}f'\left(y^{+}\right)=-\eta g'(\eta)=\frac{1}{\kappa} \qquad [1.39]$$

which necessarily implies that the left-hand and right-hand sides are constant and equal to $1/\kappa$. The integration of

equation [1.39] gives us the following logarithmic distribution:

$$f\left(y^+\right)=\frac{1}{\kappa}\ln y^+ + B \qquad [1.40]$$

and the outer distribution:

$$g\left(\eta\right)=-\frac{1}{\kappa}\ln \eta + B_{ext} \qquad [1.41]$$

The constant B_{ext} is directly linked to B by the relation:

$$B_{ext}=\bar{U}_{\infty}^{+}-\frac{1}{\kappa}\ln h^+ - B \qquad [1.42]$$

The logarithmic distribution can be interpreted as the consequence of two distinct zones, where the scales are, respectively, linked to the inner and the outer flow. This argument, which is commonly called the Izakson–Millikan–von Mises overlap, constitutes an indirect proof of the existence of the logarithmic layer. The underlying hypothesis is that the intermediary zone is independent of the Reynolds number, i.e. the function f accepts a local similarity, it is not in the form $f\left(\frac{y\bar{u}_{\tau}}{\nu}, Re\right)$. Panton [PAN 07] proceeded differently to reach a similar conclusion. He used the asymptotic Poincaré series in the outer and inner regions and rigorously overlaped them to create the composite profiles of mean velocity and the Reynolds shear stress. He clearly showed that the logarithmic law is the internal asymptote of the distribution in outer scales, and the external asymptote of the profiles in wall units.

The structure of the external layer is greatly similar to that of a wake. The structures with large scales, which depend essentially on the inertia, and depend little on the

viscosity, govern the mechanism of turbulent transport in both cases. Coles[8] proposed a velocity distribution that is valid both in the logarithmic sublayer and the outer layer, by adding a function known as a "wake function", to the distribution [1.25]:

$$\bar{U}^+\left(y^+\right)=\frac{1}{\kappa}\ln y^+ + B + \frac{\Pi}{\kappa}W_c\left(\frac{y}{\Lambda_0},\Pi\right) \qquad [1.43]$$

where the argument of the wake function W_c is the distance from the wall, rendered dimensionless by the external scale Λ_0 (the half-height h of a channel or the thickness δ of a boundary layer) and Π is a constant that depends slightly on the Reynolds number in a canonic boundary layer without pressure gradient and varies between 0.54 and 0.55. The empirical function W_c, proposed by Coles, is

$$W_c(\eta)=1+\sin\frac{(2\eta-1)\pi}{2} \qquad [1.44]$$

where $\eta=y/\Lambda_0$. The constant Π depends (slightly) on the Reynolds number in a boundary layer without pressure gradient and typically varies between 0.54 and 0.55.

Let us look again at the distribution [1.28] in outer scales. Generally speaking, this distribution depends not only on the variable $\eta=y/\Lambda_0=y/\delta$, but also on the Reynolds number, expressed as $\delta^+=\delta\bar{u}_\tau/\nu$. Thus, relation [1.28] is expressed in the general form:

$$\frac{\bar{U}_\infty-\bar{U}(y)}{\bar{u}_\tau}=g\left(\eta,\delta^+\right) \qquad [1.45]$$

8 These results were published in the first edition of the *Journal of Fluid Mechanics* (vol. 1, p. 191, 1956), a renowned journal in this field.

The displacement thickness can thus be written as

$$\delta_d = \int_0^\infty \frac{\bar{U}_\infty - \bar{U}}{\bar{U}_\infty} dy = \frac{\bar{u}_\tau}{\bar{U}_\infty} \delta \int_0^\infty g\left(\eta, \delta^+\right) d\eta$$

which leads to

$$\frac{\delta_d}{\delta} = A_1\left(\delta^+\right) \frac{\bar{u}_\tau}{\bar{U}_\infty}\left(\delta^+\right) \qquad [1.46]$$

The quantity A_1, which replaces the integral $\int_0^\infty g\left(\eta, \delta^+\right) d\eta$, depends normally on the Reynolds number δ^+. In parallel, the momentum thickness assumes the form:

$$\frac{\theta}{\delta} = \int_0^\infty \frac{\bar{U}}{\bar{U}_\infty}\left(1 - \frac{\bar{U}}{\bar{U}_\infty}\right) d\eta = \frac{\bar{u}_\tau}{\bar{U}_\infty} \int_0^\infty g\left(\eta, \delta^+\right) d\eta + \left(\frac{\bar{u}_\tau}{\bar{U}_\infty}\right)^2 \int_0^\infty g^2\left(\eta, \delta^+\right) d\eta$$

which results in

$$\frac{\theta}{\delta} = A_1 \frac{\bar{u}_\tau}{\bar{U}_\infty}\left(1 - A_2 \frac{\bar{u}_\tau}{\bar{U}_\infty}\right) \qquad [1.47]$$

with

$$A_2\left(\delta^+\right) = \int_0^\infty g^2\left(\eta, \delta^+\right) d\eta$$

The shape factor H is directly obtained from equations [1.46] and [1.47],

$$H = \frac{\delta_d}{\theta} = \left(1 - A_2 \frac{\bar{u}_\tau}{\bar{U}_\infty}\right)^{-1}$$

Equation [1.47] can be re-arranged as

$$\delta^+ = \frac{H\left(\delta^+\right)}{A_1\left(\delta^+\right)}\frac{\bar{U}_\infty \theta}{\nu} = \frac{H\left(\delta^+\right)}{A_1\left(\delta^+\right)} Re_\theta \qquad [1.48]$$

Readers are invited to consult Chapter 2 of [TAR 11a] and [TAR 11b] for further detail.

1.9. Turbulent intensities of the velocity components

The turbulent intensity of the streamwise velocity fluctuations in wall units is illustrated in Figure 1.11. We can see that the maximum value of $\sqrt{\overline{uu}}/\bar{u}_\tau$ is reached at approximately $y^+ = 15$, and it increases in line with the Reynolds number.

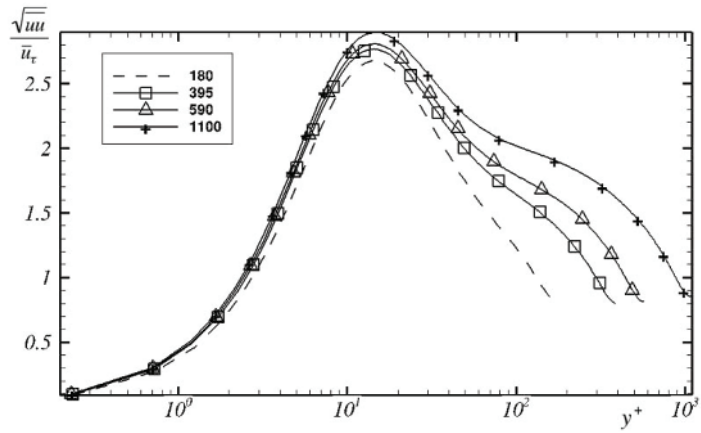

Figure 1.11. *Profiles for the turbulent intensity of the streamwise velocity fluctuations, according to the DNSs performed by Bauer [BAU 14]*

The component with the highest energy is $\sqrt{\overline{uu}}$, followed by the spanwise component $\sqrt{\overline{ww}}$ (Figure 1.13) and the wall-normal component (Figure 1.12). The mechanism of inter-

component transfer is found by way of different terms of the transport equations, as will be discussed in the next chapter.

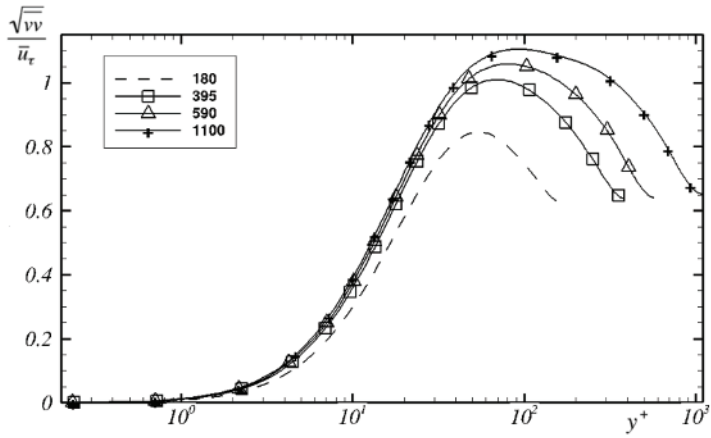

Figure 1.12. *Profiles for the turbulent intensity of the wall-normal velocity fluctuations, according to the DNSs performed by Bauer [BAU 14]*

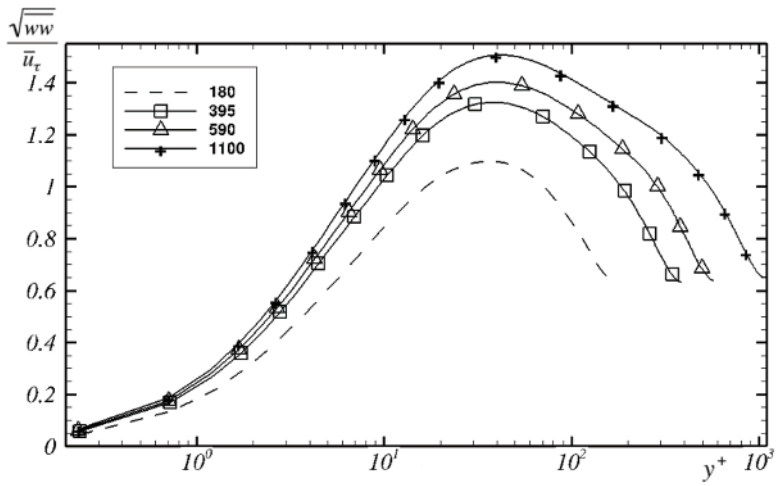

Figure 1.13. *Profiles for the turbulent intensity of the spanwise velocity fluctuations, according to the DNSs performed by Bauer [BAU 14]*

The increase in the peak of the turbulent intensities observed in Figures 1.11–1.13 suggests that the influence of the Reynolds number is not limited to the mean velocity distribution $\bar{U}\left(y^{+}\right)$, but also applies to the characteristics of the fluctuating field. For example, Figure 1.14 shows the distribution of the maximum streamwise velocity turbulent intensity as a function of the Reynolds number $Re_\tau = \bar{u}_\tau \Lambda_0 / \nu$. We can clearly see that $\left(\overline{uu}/\bar{u}_\tau^2\right)_{max}$ increases by a factor of 2 in the range $180 \le Re_\tau \le 10^6$.

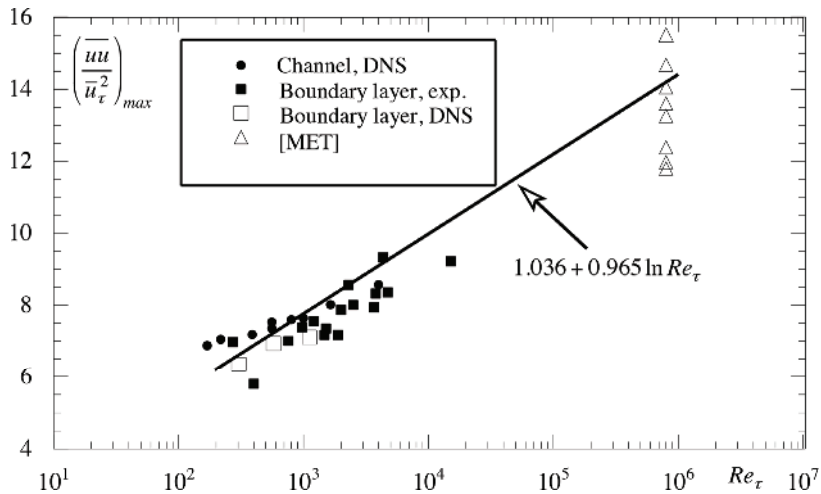

Figure 1.14. *Maximum of streamwise velocity turbulent intensity as a function of the Reynolds number. This figure is adapted from [HUT 07b]. Boundary layer (experimental): [DEG 00, UED 75, LIG 87, BAL 91, JOH 87, JOH 89, CHI 95, PUR 81]. Boundary layer, direct numerical simulations (DNSs): [SPA 88]. Channel by DNS: [ALA 01, ALA 03, ALA 04, JIM 04, MOS 99]*

The maxima of the intensities $\left(\overline{vv}/\bar{u}_\tau^2\right)_{max}$ and $\left(\overline{ww}/\bar{u}_\tau^2\right)_{max}$ also increase in approximately linear fashion with $\ln\left(Re_\tau\right)$ [TAR 11a, TAR 11b], under the influence of the passive structures discussed in [TOW 76]. These structures are

irrotational and contribute to $\overline{uu}$, $\overline{vv}$ (to a lesser degree) and $\overline{ww}$, but not to the Reynolds stress $-\overline{uv}$.[9] Thus, the effect of the Reynolds number on $-\left(\overline{uv}\right)_{max}$ is lesser, and reflects the simple fact that the constant shear stress sublayer must emerge with high Reynolds numbers. Panton [PAN 07] suggests

$$\left(-\frac{\overline{uv}}{\overline{u}_\tau^2}\right)_{\max} \propto 1-\frac{2}{\sqrt{\kappa Re_\tau}} \quad \text{for } Re_\tau \to \infty \qquad [1.49]$$

and

$$y^+_{-\overline{uv},\max} \propto \sqrt{\frac{Re_\tau}{\kappa}} \quad \text{for } Re_\tau \to \infty \qquad [1.50]$$

for the position at the wall where the Reynolds stress reaches its maximum value. Figure 1.15 recaps the experimental results analyzed by Fernholz and Finley [FER 96], and compares these measurements with the estimation [1.49] (the von Kárman constant used for the estimation is $\kappa = \kappa_{RNG} = 0.37$). We note a non-insignificant dispersion of the experimental results around $Re_\theta = 10^3$. On the other hand, the measurements are indeed grouped around relation [1.49] at $Re_\theta \geq 4\times10^3$.

9 We will see, in particular in the last chapter, that structures with large scales are, in reality, not totally passive and transport significant amounts of Reynolds shear stress in a limited area of the logarithmic sublayer, at large Re_τ values. In this chapter, however, we will content ourselves with highlighting the lesser sensitivity of $-\overline{uv}$ to Re_τ in comparison to that of the $\overline{u_i u_i}$, and presenting the classical points of view, without lingering on the topic of the recent advances, which will be discussed in subsequent chapters.

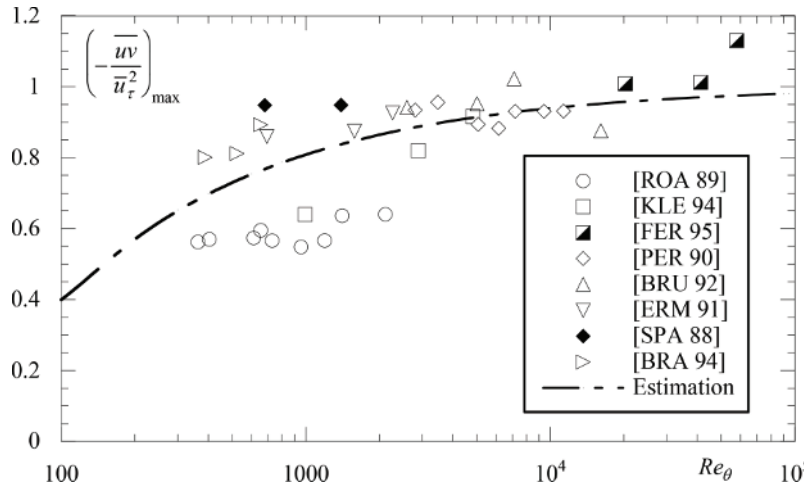

Figure 1.15. *Distributions of the maximum value of the Reynolds stress in external (boundary layer) flows. This figure is adapted from [FER 96]. The estimation is based on relation [1.49]. See [TAR 11b] for further detail*

Approaches based on the spectral behaviors and the effects of the attached structures found by Townsend [TOW 76] are in agreement, yielding the logarithmic distributions of the intensities $\overline{uu}$ and $\overline{ww}$ in the constant stress sublayer. Readers are invited to consult Chapters 3 and 4 of [TAR 11a] and [TAR 11b] for the details and the many references related to these aspects. In summary, the turbulent intensities in the fully turbulent zone are expressed as:

$$\begin{aligned}
&\frac{\overline{uu}}{\overline{u}_\tau^2}\left(y^+\right) = -A_{uu}\ln\frac{y}{\Lambda_0} + B_{uu}\\
&\frac{\overline{vv}}{\overline{u}_\tau^2}\left(y^+\right) = B_{vv}\\
&\frac{\overline{ww}}{\overline{u}_\tau^2}\left(y^+\right) = -A_{ww}\ln\frac{y}{\Lambda_0} + B_{ww}
\end{aligned} \qquad [1.51]$$

These distributions attain their asymptotic form with universal constants within the limit of large Reynolds numbers, in the zone with no viscous effect, where the total stress is reduced to the Reynolds stress – in other words, in the logarithmic sublayer delimited by $3\sqrt{Re_\tau} \le y^+ \le 0.15Re_\tau$ [EYI 08, KLE 09, MAR 13]. The coefficient A_{uu} is then 1.26 [MAR 13]. Figure 1.16 shows the experimental profiles of $\overline{uu}/\overline{u}_\tau^2\left(y^+\right)$ across a wide range of large Reynolds numbers. The emergence of the logarithmic distribution with a "universal" constant A_{uu} is clearly visible.

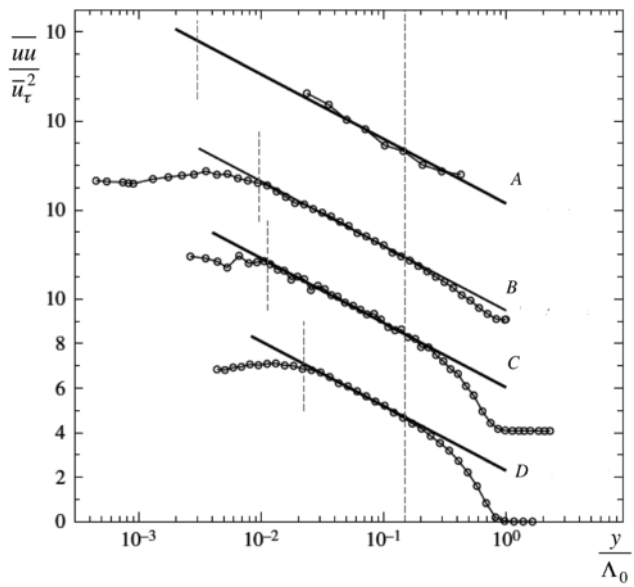

Figure 1.16. *Distributions of the turbulent intensity of the streamwise velocity for* $Re_\tau = 628,000$ *(A),* $98,190$ *(B),* $68,780$ *(C),* $18,010$ *(D). The vertical dotted lines delimit the zone* $3\sqrt{Re_\tau} \le y^+ \le 0.15Re_\tau$. *This figure is adapted from [MAR 13]*

Various semi-empirical corrections can be made to relations [1.51], in particular to take account of the viscous effects with lower Reynolds numbers [TAR 11a, TAR 11b].

We can see that the streamwise and spanwise intensities behave in a similar manner, while the turbulent intensity of the wall-normal velocity fluctuations is constant, essentially because of the impermeability. A recent study conducted by Meneveau and Marusic [MEN 13] revealed that the moments of order $2p$ of the fluctuations of $u(t)$ (and probably also $w(t)$) also respect a logarithmic distribution, with

$$\frac{\left[\overline{u^{2p}}\right]^{1/p}}{\overline{u}_\tau^2}\left(y^+\right) \propto -A_p \ln\frac{y}{\Lambda_0} \qquad [1.52]$$

where p is an integer.

1.10. Fine structure

Analyzing the third- and fourth-order moments of the fluctuating quantities is a classic statistical analysis method, commonly used in wall turbulence. The third-order moment of a normalized fluctuating quantity q is the skewness factor, defined by

$$S(q) = \frac{\overline{q^3}}{\left(\overline{q^2}\right)^{3/2}} \qquad [1.53]$$

The skewness factor is null for any normalized random variable with symmetrical probability density function. Thus, positive or negative values of S_q are, therefore, precursors of the probability density's shifting, respectively, toward $q > 0$ and $q < 0$.

The odd-order moments of the spanwise component are null in a fully developed turbulent channel flow, because of the reflectional invariance with respect to the spanwise

direction.[10] Consequently, $S(w)=0$, as shown in Figure 1.17(c). The skewness factor $S(u)$ attains values close to 1 near to the wall, and tends toward $S(u)=-0.5$ at the centerline, irrespective of the Reynolds number, within the range $180<Re_\tau<1{,}100$. The dissymmetry of the wall-normal velocity fluctuations is positive in the viscous and logarithmic sublayers and $S(v)<0$ in the buffer sublayer (Figure 1.17(b)). The profiles of the third- and fourth-order moments with $Re_\tau=180$ correspond closely to the results recently published in [VRE 14].

The fourth-order moment is a measure of intermittence. Its dimensionless form

$$F(q)=\frac{\overline{q^4}}{\left(\overline{q^2}\right)^2} \qquad [1.54]$$

is called the flatness (kurtosis) factor. The kurtosis of a random Gaussian variable is 3. Figure 1.18 shows that the F factor of the three velocity components approaches this value near the centerline, though never completely reaches it. The exception is the spanwise velocity with $S(w)=0$ and $F(w)=3$ in a relatively extensive area of the outer layer (Figure 1.18(c)). The normal component v is most intermittent near to the wall, and $F(v)$ clearly increases with the Reynolds number, as shown in Figure 1.18(b), reaching values as high as $F(v)=42$ at $Re_\tau=1{,}100$ at $y^+\to 0$. Then comes the spanwise component w, whose flatness factor is near to 10 in a layer adjacent to the wall.

10 See section 2.2.

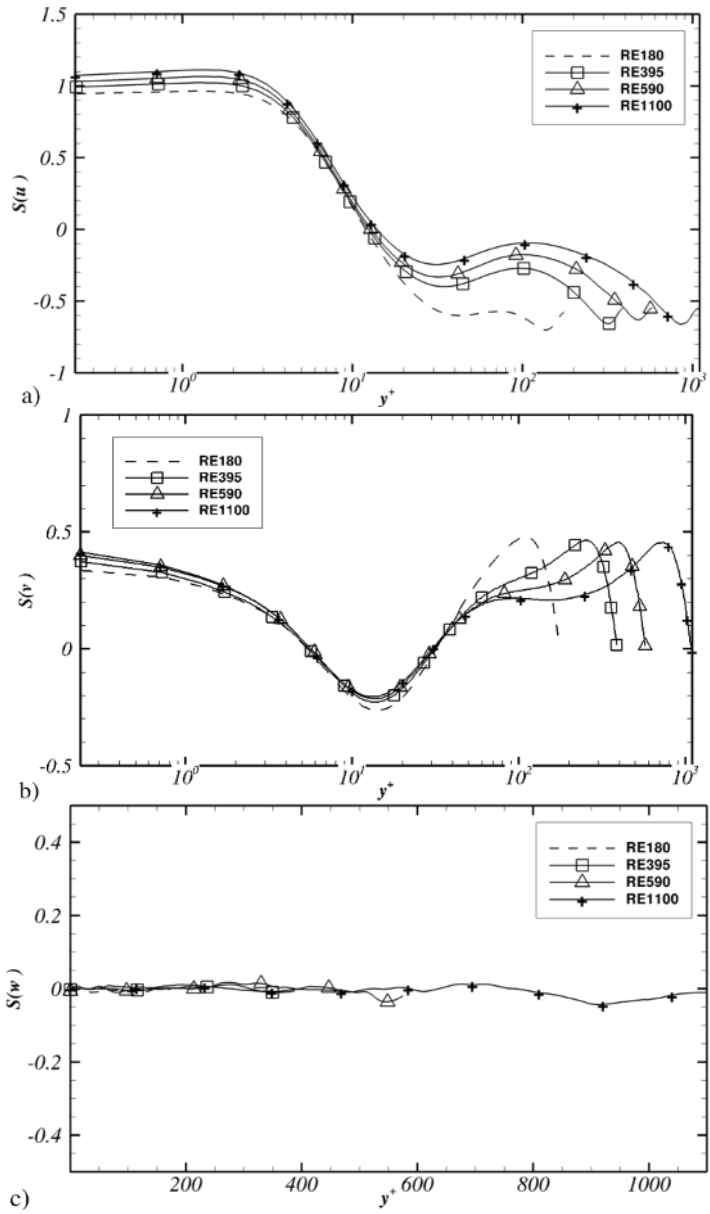

Figure 1.17. *Distribution of the skewness of the a) streamwise velocity fluctuations, b) wall-normal velocity fluctuations and c) spanwise velocity fluctuations according to the DNSs performed by Bauer [BAU 14]*

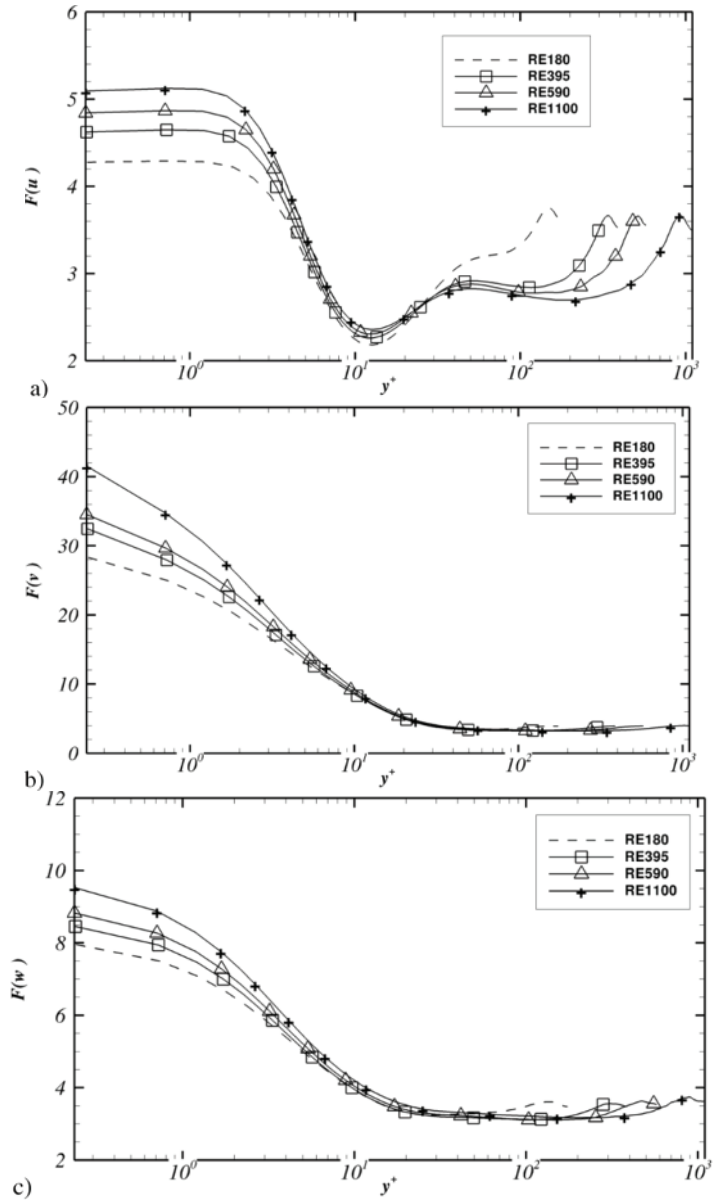

Figure 1.18. *Distribution of flatness factor of a) streamwise, b) wall-normal and c) spanwise velocity fluctuations according to the DNSs performed by Bauer [BAU 14]*

1.11. Vorticity

Chapter 5 of [TAR 11a] and [TAR 11b] is entirely devoted to the characteristics of the vorticity field near to the wall. We will briefly summarize certain aspects here because the generation of near-wall coherent structures is closely linked to the dynamics of the vorticity, and in particular to its streamwise component ω_x. The vorticity is the rotational $\vec{\omega} = \vec{\nabla} \wedge \vec{u}$ of the velocity field. The transport equations for ω_i are thus obtained by applying the rotational to the momentum balance equations (which eliminates the pressure terms). The transport equation for the instantaneous vorticity field thus obtained is

$$\frac{D\left(\bar{\Omega}_i + \omega_i\right)}{Dt} = \left(\bar{\Omega}_j + \omega_j\right)\frac{\partial}{\partial x_j}\left(\bar{U}_i + u_i\right) + \nu\frac{\partial^2}{\partial x_l \partial x_l}\left(\bar{\Omega}_i + \omega_i\right) \quad [1.55]$$
$$= P_{\omega_i} + D_{\omega_i}$$

where the choice of indicial notation enables us to make use of the Einstein convention of summation over the repeated indices. The component $\bar{\Omega}_i(\vec{x}) = \left[\vec{\nabla} \wedge \vec{U}(\vec{x})\right]_i$ corresponds to the average vorticity and $\omega_i(\vec{x},t) = \left[\vec{\nabla} \wedge \vec{u}(\vec{x},t)\right]_i$ represents the fluctuating component. The left-hand term in equation [1.55] contains the inertial terms. The first term on the right-hand side represents the terms of vorticity production P_{ω_i}, which are of crucial importance in the dynamics of wall turbulence, and which we will discuss in detail later on. The last term in equation [1.55] represents the diffusion D_{ω_i} of $\bar{\Omega}_i(\vec{x}) + \omega_i(\vec{x},t)$. The mean vorticity in a fully developed turbulent channel flow, homogeneous in the streamwise and

spanwise directions (respectively, $x(i=1)$ and $z(i=3)$), is nothing but the spanwise component $\bar{\Omega}_z(y) = -d\bar{U}/dy$. We have

$$\bar{\Omega}_z(x,y) = \partial\bar{V}/\partial x - \partial\bar{U}/\partial y$$

in a canonical turbulent boundary layer on an infinite flat plate. Given that the order of magnitude of $\partial\bar{V}/\partial x$ is lesser than that of the shear $\partial\bar{U}/\partial y$, the average spanwise component is approximately $\bar{\Omega}_z(x,y) \approx -\partial\bar{U}/\partial y$ in these conditions.

The components of the fluctuating vorticity field are:

$$\begin{aligned}
\omega_x(x,y,z,t) &= \frac{\partial w}{\partial y} - \frac{\partial v}{\partial z} \\
\omega_y(x,y,z,t) &= \frac{\partial u}{\partial z} - \frac{\partial w}{\partial x} \\
\omega_z(x,y,z,t) &= \frac{\partial v}{\partial x} - \frac{\partial u}{\partial y}
\end{aligned} \qquad [1.56]$$

respectively, in the streamwise, wall-normal and spanwise directions. The vector form of the transport equation [1.55] is useful, particularly if we want to express that equation in the general curvilinear coordinates,

$$\frac{\partial\vec{\omega}}{\partial t} + \vec{u}\bullet\vec{\nabla}\vec{\omega} = \left(\vec{\omega}\bullet\vec{\nabla}\right)\vec{u} + \nu\nabla^2\vec{\omega} \qquad [1.57]$$

where the details of the decomposition into an average and fluctuating value are deliberately omitted for the sake of conciseness. In order to save the readers from needlessly wasting time, we now briefly recap the vectorial operators appearing in the above expression in a curvilinear coordinates system $(\vec{e}_1, \vec{e}_2, \vec{e}_3)$ and the transformations

$x = x(x_1, x_2, x_3)$, $y = y(x_1, x_2, x_3)$ and $z = z(x_1, x_2, x_3)$. The metric coefficients are

$$h_i = \sqrt{\left(\frac{\partial x}{\partial x_i}\right)^2 + \left(\frac{\partial y}{\partial x_i}\right)^2 + \left(\frac{\partial z}{\partial x_i}\right)^2} \qquad [1.58]$$

for $i = 1, 2$ and 3. The gradient is expressed by

$$\vec{\nabla} = \frac{\vec{e}_1}{h_1}\frac{\partial}{\partial x_1} + \frac{\vec{e}_2}{h_2}\frac{\partial}{\partial x_2} + \frac{\vec{e}_3}{h_3}\frac{\partial}{\partial x_3} \qquad [1.59]$$

The rotational (and the vorticity) in the system $(\vec{e}_1, \vec{e}_2, \vec{e}_3)$ is

$$\vec{\omega} = \omega_1\vec{e}_1 + \omega_2\vec{e}_2 + \omega_3\vec{e}_3 = \vec{\nabla} \wedge \vec{u} = \begin{vmatrix} h_1\vec{e}_1 & h_2\vec{e}_2 & h_3\vec{e}_3 \\ \dfrac{\partial}{\partial x_1} & \dfrac{\partial}{\partial x_2} & \dfrac{\partial}{\partial x_3} \\ h_1u_1 & h_2u_2 & h_3u_3 \end{vmatrix} \qquad [1.60]$$

The operator ∇^2 is expressed by

$$\nabla^2\vec{\omega} = \frac{1}{h_1h_2h_3}\left[\frac{\partial}{\partial x_1}\left(\frac{h_2h_3}{h_1}\frac{\partial\vec{\omega}}{\partial x_1}\right) + \frac{\partial}{\partial x_2}\left(\frac{h_1h_3}{h_2}\frac{\partial\vec{\omega}}{\partial x_2}\right) + \frac{\partial}{\partial x_3}\left(\frac{h_1h_2}{h_3}\frac{\partial\vec{\omega}}{\partial x_3}\right)\right] \qquad [1.61]$$

Let us supplement these relations with the expression of the divergence, which could be applied, for example, to the velocity vector $\vec{u}(x_1, x_2, x_3; t)$

$$\vec{\nabla} \bullet \vec{u} = \frac{1}{h_1h_2h_3}\left[\frac{\partial h_2h_3u_1}{\partial x_1} + \frac{\partial h_1h_3u_2}{\partial x_2} + \frac{\partial h_1h_2u_3}{\partial x_3}\right] \qquad [1.62]$$

The vorticity transport equation in the curvilinear coordinates will be used (although not frequently) in

Chapter 5. The vectorial forms enable us to easily transform any transport equation in any curvilinear system.

1.11.1. *Characteristics of vorticity field near to the wall*

The generic structures of wall turbulence are the quasi-streamwise vortices (QSVs) responsible for turbulent production and mixing. The streamwise vorticity in the direction of the flow is of capital importance for these reasons, and is worthy of a separate comment even at this early stage. The instantaneous transport equation for the streamwise vorticity can be easily obtained on the basis of equation [1.55]:

$$\frac{D\omega_x}{Dt}=\omega_x\frac{\partial u}{\partial x}+\omega_y\frac{\partial\left(\bar{U}+u\right)}{\partial y}+\left(\omega_z+\bar{\Omega}_z\right)\frac{\partial u}{\partial z}+\nu\frac{\partial^2}{\partial x_l\,\partial x_l}\omega_x \quad [1.63]$$

for a fully developed channel flow homogeneous in x and z. The first three terms on the right in equation [1.63] correspond to the production terms. The term $\omega_x\partial u/\partial x$ represents production by stretching of the material lines of vorticity by the instantaneous local gradient $\partial u/\partial x$. The elongation of the material line of vorticity by stretching increases the intensity of that vorticity, as predicted by Kelvin's theorem. Production by tilting of wall-normal vorticity ω_y by the local shear gives rise to $\omega_y\partial\left(\bar{U}+u\right)/\partial y$, while the spanwise component ω_z creates ω_x by rotation around $\left(\omega_z+\bar{\Omega}_z\right)\partial u/\partial z$. The three mechanisms of production are shown schematically in Figure 1.19.

By combining and simplifying equations [1.56] and [1.63], we find:

$$\frac{D\omega_x}{Dt}=\left(\frac{\partial w}{\partial y}-\frac{\partial v}{\partial z}\right)\frac{\partial u}{\partial x}-\frac{\partial w}{\partial x}\frac{\partial\left(\bar{U}+u\right)}{\partial y}+\frac{\partial v}{\partial x}\frac{\partial u}{\partial z}+\nu\frac{\partial^2\omega_x}{\partial x_l\,\partial x_l} \quad [1.64]$$

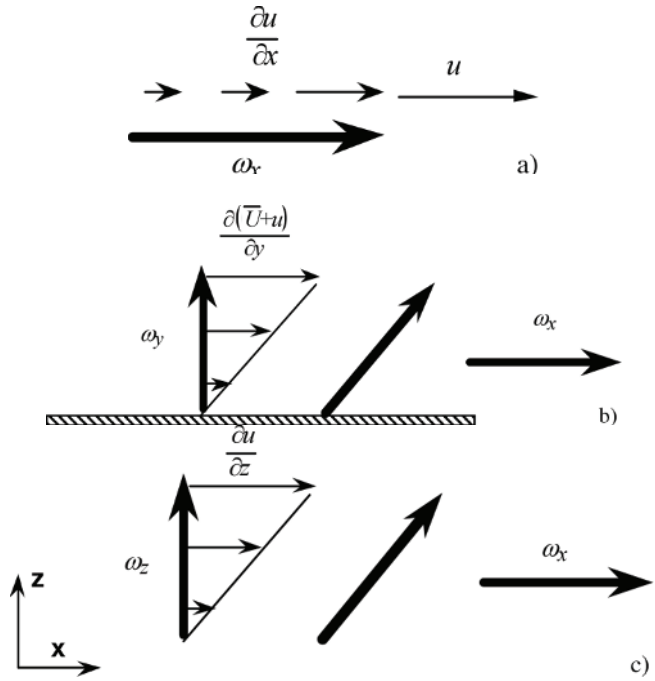

Figure 1.19. *Mechanisms of vorticity production in a canonical turbulent wall flow. a) Production by stretching: the local and instantaneous streamwise gradient pulls the vortex cores, which become more intense. b) Production by tilting of the wall-normal vorticity by the local shear. c) Production by rotation of the spanwise component and the spanwise gradient of the local streamwise velocity component of the velocity*

There are two interesting aspects in this relation. First, we can see that after simplification, the term representing production by tilting is reduced to

$$P_{I\omega_x} = -\frac{\partial w}{\partial x}\frac{\partial\left(\bar{U}+u\right)}{\partial y}$$

where the subscript I denotes the tilting. A simple analysis of the order of magnitude of the production terms also

reveals that the dominant terms are those that contain the mean shear $\partial \bar{U}/\partial y$. Put differently

$$P_{\omega_x} \approx P_{I\omega_x} \approx -\frac{\partial w}{\partial x}\frac{\partial \bar{U}}{\partial y}$$

In other words, streamwise vorticity production is essentially due to the tilting of the shear layers $\partial w/\partial x$. The spanwise structure, therefore, plays a very significant role. The process of regeneration of the layers $\partial w/\partial x$ is complex and will be analyzed in detail in Chapter 5. The mean vorticity at the wall runs in the spanwise direction and is nothing but

$$\bar{\Omega}_{z0} = -\left(\frac{\partial \bar{U}}{\partial y}\right)_0 = -\frac{\bar{\tau}_x}{\mu} = -\frac{\bar{\tau}_0}{\mu} = -\frac{\bar{u}_\tau^2}{\nu} \qquad [1.65]$$

where the subscript 0, as usual, refers to the wall and $\bar{\tau}_0$ is the mean wall shear stress (in the direction of the mean flow). Two fluctuating vorticity components in the streamwise and spanwise directions, respectively, remain at the wall:

$$\begin{aligned}
\omega_{x0}(x,z,t) &= \left(\frac{\partial w}{\partial y}\right)_0 = \frac{\tau_z'(x,z,t)}{\mu} = \frac{\tau_z'(x,z,t)}{\mu} \\
\omega_{z0}(x,z,t) &= \left(-\frac{\partial u}{\partial y}\right)_0 = -\frac{\tau_x'(x,z,t)}{\mu} = -\frac{\tau_x'(x,z,t)}{\mu} = -\frac{\tau_0'}{\mu}
\end{aligned} \qquad [1.66]$$

whereas $\omega_{y0} = 0$. The turbulent intensity $\overline{\tau_0'\tau_0'}$ of the wall shear stress is directly linked to $\overline{\omega_{z0}\omega_{z0}}$. We have precisely:

$$\left(\sqrt{\overline{\tau_0'\tau_0'}}\right)^+ = \sigma_{\tau_x'}^+ = \frac{\sqrt{\overline{\tau_0'\tau_0'}}}{\overline{\tau}_0} = \frac{\sqrt{\overline{\omega_{z0}\omega_{z0}}}}{\overline{\Omega}_{z0}} = \left(\sqrt{\overline{\omega_{z0}\omega_{z0}}}\right)^+ = \sigma_{\omega_{z0}}^+$$
$$\left(\sqrt{\overline{\tau_z'\tau_z'}}\right)^+ = \sigma_{\tau_z'}^+ = \frac{\sqrt{\overline{\omega_{x0}\omega_{x0}}}}{\overline{\Omega}_{z0}} = \sigma_{\omega_{x0}}^+ \qquad [1.67]$$

in inner scales. The value σ_q corresponds to the quadratic mean of q.[11] Considering the asymptotic behaviors of the mean velocity and the fluctuations of velocity near to the wall:

$$\overline{U}(y) = \left(\frac{\partial \overline{U}}{\partial y}\right)_0 y + O\left(y^2\right)$$
$$u = \left(\frac{\partial u}{\partial y}\right)_0 y + O\left(y^2\right)$$
$$w = \left(\frac{\partial w}{\partial y}\right)_0 y + O\left(y^2\right)$$

where $O(\ )$ indicates terms of order greater than y, it is easy to show that:

$$\sigma_{\tau_x'}^+ = \lim_{y\to 0} \frac{\sqrt{\overline{uu}}}{\overline{U}}$$
$$\sigma_{\tau_z'}^+ = \lim_{y\to 0} \frac{\sqrt{\overline{ww}}}{\overline{U}} \qquad [1.68]$$

The statistics on the fluctuating wall shear stress can, therefore, be determined on the basis of the velocity field near to the wall. However, this requires us to determine (either experimentally or by precise direct numerical

11 For the sake of conciseness, the quantities σ_q and the variance σ_q^2 will be used indiscriminately to denote the turbulent intensity of q.

simulations) the fluctuating components in the viscous sublayer, also at distances very near to the walls ($y^+ \leq 2$).

Let us now consider the instantaneous and local momentum balance equations directly at the wall. In a canonical flow in the absence of any action exerted at the walls (such as distributed blowing/suction for example), these equations can be written as

$$\left[\frac{D}{Dt}\left(\overline{U}_i + u_i\right)\right]_0 = 0 = -\frac{1}{\rho}\frac{\partial}{\partial x_i}\left(\overline{P} + p\right)_0 + \nu\frac{\partial^2}{\partial x_l \partial x_l}\left(\overline{U}_i + u_i\right)_0$$

Noting that the diffusion terms can be expressed as:

$$\nu\frac{\partial^2}{\partial x_l \partial x_l}\left(\overline{U}_i + u_i\right) = -\nu\varepsilon_{ijk}\frac{\partial}{\partial x_j}\left(\overline{\Omega}_k + \omega_k\right)$$

we obtain:

$$\frac{\partial}{\partial x_i}\left(\overline{P} + p\right)_0 = -\mu\varepsilon_{ijk}\frac{\partial}{\partial x_j}\left(\overline{\Omega}_k + \omega_k\right)_0$$

which finally gives us

$$\begin{aligned}\frac{\partial}{\partial x}(p)_0 &= -\mu\left(\frac{\partial \omega_z}{\partial y}\right)_0 \\ \frac{\partial}{\partial z}(p)_0 &= -\mu\left(\frac{\partial \omega_x}{\partial y}\right)_0\end{aligned} \qquad [1.69]$$

This relation clearly indicates that the fluxes of fluctuating spanwise and streamwise components of vorticity are directly linked to the instantaneous and local pressure gradients at the wall, respectively, in the directions x and z. Equation [1.69] is accurate, and it is at the heart of certain strategies for controlling wall turbulence. It is easy to see

that the wall flux of mean vorticity $\bar{\Omega}_z$ is linked to $\dfrac{\partial \bar{P}}{\partial x}$ along $\partial \bar{P}/\partial x = -\mu\left(\partial \bar{\Omega}_z/\partial y\right)_0$ in a turbulent channel flow, homogenous in x and z. In a boundary layer on a flat plate, on the other hand, $\left(\partial \bar{\Omega}_z/\partial y\right)_0 = 0$ since the average pressure gradient is then null because of the boundary layer approximation. Equation [1.69], which relates to the fluctuating fields, of course remains valid in this latter case.

The momentum balance equations at the wall give no indication about the wall flux of wall-normal vorticity $\left(\partial \omega_y/\partial y\right)_0$, which may not necessarily be zero although strictly speaking, $\omega_{y0} = 0$. Indeed, we actually have:

$$\vec{\nabla} \bullet \vec{\omega} = \vec{\nabla} \bullet \left(\vec{\nabla} \wedge \vec{u}\right) = 0$$

which implies

$$\left(\frac{\partial \omega_y}{\partial y}\right)_0 = -\left(\frac{\partial \omega_x}{\partial x} + \frac{\partial \omega_z}{\partial z}\right)_0$$

and there is no reason for the flow $\left(\partial \omega_y/\partial y\right)_0$ to become null locally and instantaneously.

The wall is a source of vorticity. The vorticity is created at the wall and subsequently diffuses. It is then advected and regenerated in a highly 3D environment. The transfer of vorticity from one component to another is perpetually occurring during this process. The dominant component of vorticity *near* to the wall is in the spanwise

direction, $\bar{\Omega}_z(\vec{x}) + \omega_z(\vec{x},t)$. If we now consider the evolution of the wall-normal vorticity component, we have

$$\frac{D\omega_y}{Dt} = \omega_x \frac{\partial v}{\partial x} + \omega_y \frac{\partial v}{\partial y} + \left(\omega_z + \bar{\Omega}_z\right)\frac{\partial v}{\partial z} + \nu \frac{\partial^2 \omega_y}{\partial x_l \partial x_l} \qquad [1.70]$$

which can be simplified as:

$$\frac{D\omega_y}{Dt} = \left(\frac{\partial v}{\partial x}\frac{\partial w}{\partial y}\right) + \left(\frac{\partial u}{\partial z} - \frac{\partial w}{\partial x}\right)\frac{\partial v}{\partial y}$$
$$+ \left(\bar{\Omega}_z - \frac{\partial u}{\partial y}\right)\frac{\partial v}{\partial z} + \nu \frac{\partial^2}{\partial x_l \partial x_l}\omega_y$$

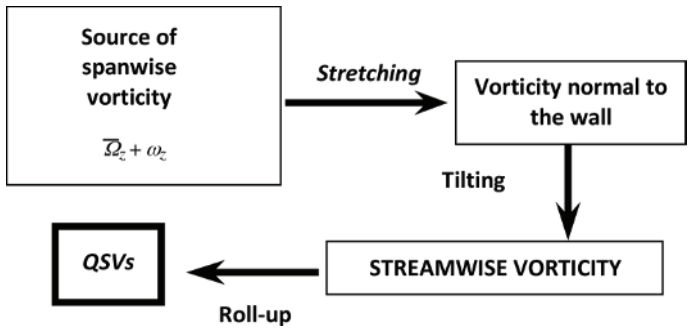

Figure 1.20. *Transfer of the spanwise vorticity component into wall-normal and streamwise vorticity in the inner sublayer of a turbulent wall flow. The local zones of streamwise vorticity may roll up into coherent quasi-streamwise vortices (QSVs)*

A simple analysis of the order of magnitude is sufficient to show that the predominant production term of ω_y is $\bar{\Omega}_z \partial v/\partial z$ in the inner sublayer, where $\bar{\Omega}_z^+ \approx 1$, which is nothing but the stretching of the spanwise vorticity $\bar{\Omega}_z$ by the shear $\partial v/\partial z$. We can, therefore, suggest a simplified physical image of the dynamics of vorticity in the buffer sublayer. The normal vorticity is null at the wall, but is

created by the stretching of the spanwise vorticity in immediate proximity. It is then tilted, again because of the mean shear, to create the streamwise component ω_x, which can "roll up" and develop into QSVs that play a fundamental role in the structure of the wall turbulence, and constitutes the main subject of this book. This suggestion is represented in Figure 1.20.

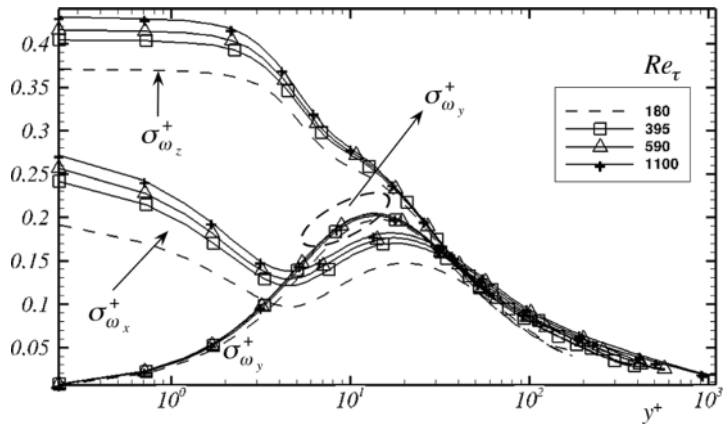

Figure 1.21. *Turbulent intensities of the spanwise, wall-normal and streamwise vorticity components in a fully developed turbulent channel flow for* $180 < Re_\tau < 1{,}100$*, respectively, according to Bauer [BAU 14]. The turbulent intensities of the spanwise and streamwise components increase with the Reynolds number, whereas the intensity of the wall-normal component is remarkably immune to variations in* Re_τ*. Also see [GIR 06]*

1.11.2. *Turbulent intensities of the fluctuating vorticity components*

Figure 1.21 shows the distribution of turbulent intensities of the vorticity components in the range $180 < Re_\tau < 1{,}100$ arising from our own direct numerical simulations [BAU 14] and corresponding closely to the results found by [HOY 08]. The intensities of the streamwise and spanwise components increase in line with the Reynolds number, particularly in the buffer sublayer. However, the intensity $\sigma^+_{\omega_y}$ remains

remarkably insensitive to Re_τ for reasons that have not yet been elucidated. One of the plausible arguments is that this insensitivity arises from the universality of the spatial distribution of the QSVs in the buffer sublayer. The wall-normal vorticity is dominated by the term $\omega_y \propto \partial u/\partial z$ at $y^+ \leq 15$, particularly near to the vortex structures, where the $\partial u/\partial z$ shear layers are engendered by purely kinematic effects. They form *thin walls* of vorticity separating the QSVs. We can, therefore, consider the fact that $\omega_y^+ \propto \partial u^+ \big/ \partial z^+ \propto u_{\omega_y}^+ \big/ \lambda_z^+$, where $u_{\omega_y}^+$ is the velocity scale linked to ω_y^+ and λ_z^+, is the spanwise spacing between the QSVs (directly linked to the spacing of the high- and low-velocity streaks, as we will see later on). It occurs that λ_z^+ depends only slightly on Re_τ, which could, in part, explain why $\sigma_{\omega_y}^+$ is independent of the Reynolds number, if only for $Re_\tau \leq 1{,}100$.